Soft and Hard X-Ray Microscopy

David Attwood
University of California, Berkeley

Cheiron School
September 2011
SPring-8

1 CheironSchool_Sept2011_Lec3.ppt

The short wavelength region of the electromagnetic spectrum

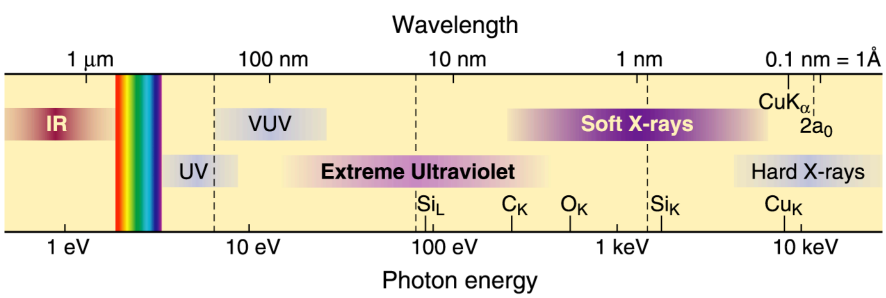

- **See smaller features**
- **Write smaller patterns**
- **Elemental and chemical sensitivity**

$$\hbar\omega \cdot \lambda = hc = 1239.842 \text{ eV nm}$$

$$n = 1 - \delta + i\beta \qquad \delta, \beta << 1$$

2 CheironSchool_Sept2011_Lec3.ppt

Two common soft x-ray microscopes

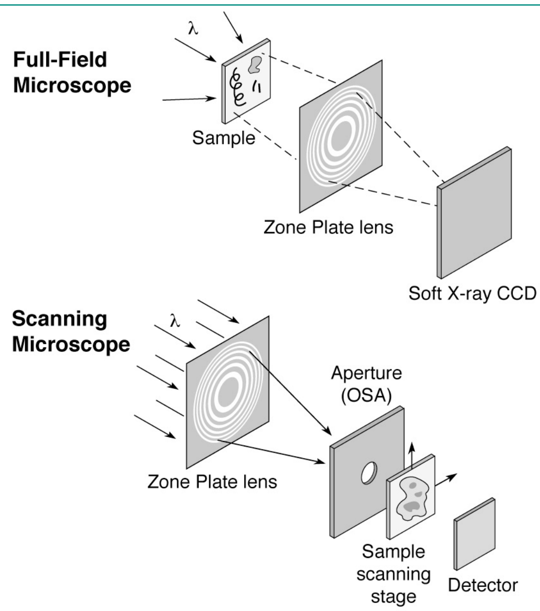

- 10–20 nm spatial resolution
- Modest spectral resolution
- Seconds exposure time
- Bending magnet radiation
- Higher radiation dose
- Flexible sample environment (wet, cryo, labeled magnetic fields, electric fields, cement, ...)

- 10–20 nm spatial resolution
- Least radiation dose
- Best spectral resolution
- Requires spatially coherent radiation
- Minutes exposure time
- Flexible sample environment
- Photoemission, fluorescence imaging

Ch09_F21_Sept2010.ai

3
CheironSchool_Sept2011_Lec3.ppt

A Fresnel zone plate lens for x-ray microscopy

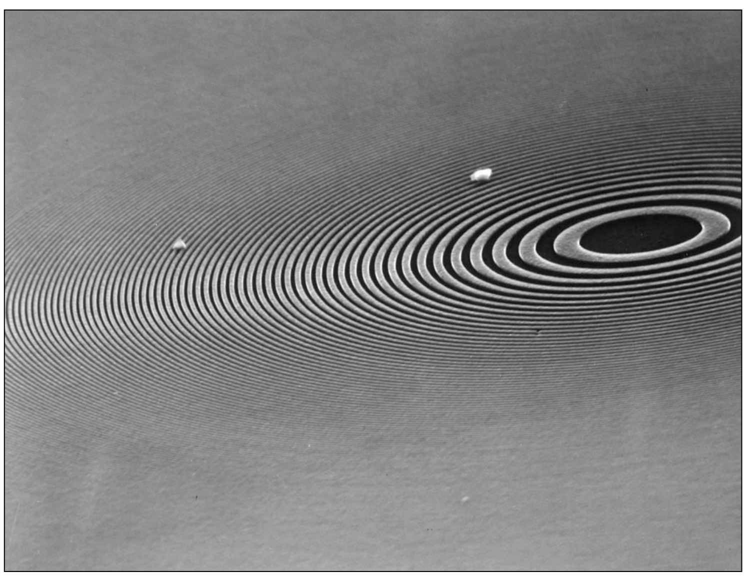

Erik Anderson, LBNL

4
CheironSchool_Sept2011_Lec3.ppt

Nature Vol 435|30 June 2005|doi:10.1038/nature-3719

LETTERS

Soft X-ray microscopy at a spatial resolution better than 15 nm

Weilun Chao[1,2], Bruce D. Harteneck[1], J. Alexander Liddle[1], Erik H. Anderson[1] & David T. Attwood[1,2]

Analytical tools that have spatial resolution at the nanometre scale are indispensable for the life and physical sciences. It is desirable that these tools also permit elemental and chemical identification on a scale of 10 nm or less, with large penetration depths. A variety of techniques[1–7] in X-ray imaging are currently being developed that may provide these combined capabilities. Here we report the achievement of sub-15-nm spatial resolution with a soft X-ray microscope—and a clear path to below 10 nm—using an overlay technique for zone plate fabrication. The microscope covers a spectral range from a photon energy of 250 eV (~5 nm wavelength) to 1.8 keV (~0.7 nm), so that primary K and L atomic resonances of elements such as C, N, O, Al, Ti, Fe, Co and Ni can be probed. This X-ray microscopy technique is therefore suitable for a wide range of studies: biological imaging in the water window[8,9]; studies of wet environmental samples[10,11]; studies of magnetic nanostructures with both elemental and spin-orbit sensitivity[12–14]; studies that require viewing through thin windows, coatings or substrates (such as buried electronic devices in a silicon chip[15]); and three-dimensional imaging of cryogenically fixed biological cells[9,16].

The microscope XM-1 at the Advanced Light Source (ALS) in Berkeley[17] is schematically shown in Fig. 1. The microscope type is similar to that pioneered by the Göttingen/BESSY group (ref. 18, and references therein). A 'micro' zone plate (MZP) projects a full-field image to an X-ray-sensitive CCD (charge-coupled device), typically in one or a few seconds, often with several hundred images per day. The field of view is typically 10 μm, corresponding to a magnification of 2,500. The condenser zone plate (CZP), with a central stop, serves two purposes in that it provides partially coherent hollow-cone illumination[2], and, in combination with a pinhole, serves as the monochromator. Monochromatic radiation of $\lambda/\Delta\lambda = 500$ is used. Both zone plates are fabricated in-house, using electron beam lithography[19].

The spatial resolution of a zone plate based microscope is equal to $k_1\lambda/NA_{MZP}$, where λ is the wavelength, NA_{MZP} is the numerical aperture of the MZP, and k_1 is an illumination dependent constant, which ranges from 0.3 to 0.61. For a zone plate lens used at high magnification, $NA_{MZP} = \lambda/2\Delta r_{MZP}$, where Δr_{MZP} is the outermost (smallest) zone width of the MZP[20]. For the partially coherent illumination[21,22] used here, $k_1 \approx 0.4$ and thus the theoretical resolution is $0.8\Delta_{MZP}$, as calculated using the SPLAT computer program[23] (a two-dimensional scalar diffraction code, which evaluates partially coherent imaging). In previous results with a $\Delta r_{MZP} = 25$ nm zone plate, we reported[2] an unambiguous spatial resolution of 20 nm. Here we describe the use of an overlay nanofabrication technique that allows us to fabricate zone plates with finer outer zone widths, to $\Delta r_{MZP} = 15$ nm, and to achieve a spatial resolution of below 15 nm, with clear potential for further extension.

This technique overcomes nanofabrication limits due to electron beam broadening in high feature density patterning. Beam broadening results from electron scattering within the recording medium (resist), leading to a loss of image contrast and thus resolvability for

$\lambda = 1.52$ nm (815 eV)
$\Delta r = 15$ nm
$N = 500$
$D = 30$ μm
$f = 300$ μm
$\sigma = 0.38$
$0.8\,\Delta r = 12$ nm

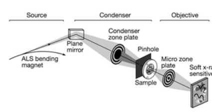

Figure 1 | A diagram of the soft X-ray microscope XM-1. The microscope uses a micro zone plate to project a full field image onto a CCD camera that is sensitive to soft X-rays. Partially coherent, hollow-cone illumination of the sample is provided by a condenser zone plate. A central stop and a pinhole provide monochromatization.

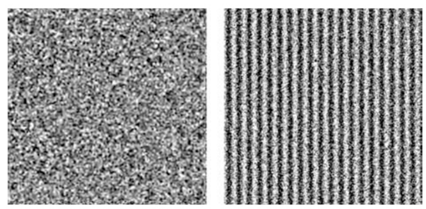

Figure 4 | Soft X-ray images of a 15.1 nm half-period test object, as formed with zone plates having outer zone widths of 25 nm and 15 nm.

Cr/Si test pattern (Cr L_3 @ 574 eV)
(2000 X 2000, 10^4 ph/pixel)

[1]Center for X-ray Optics, Lawrence Berkeley National Laboratory, 1 Cyclotron Road, MS 2-400, [2]Department of Electrical Engineering California, Berkeley, California 94720, USA.

Novel zone plates for specific functionality

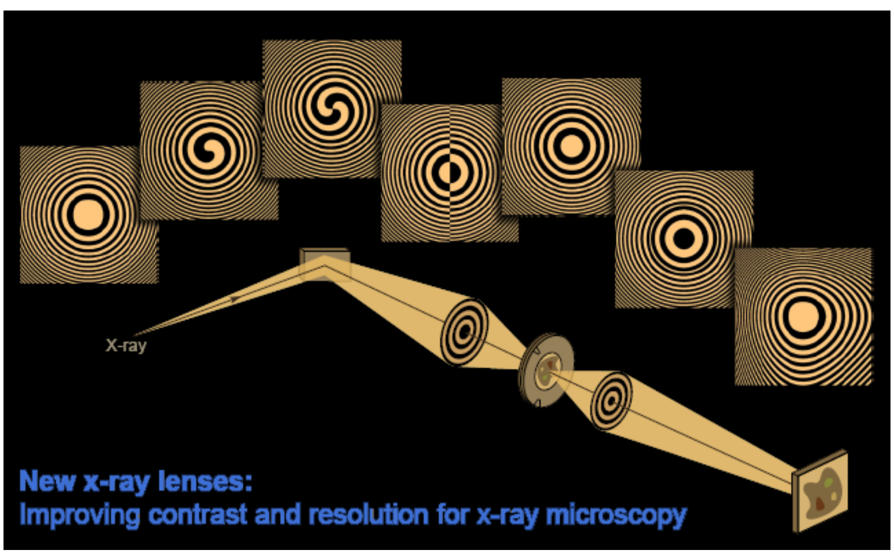

Courtesy of Anne Sakdinawat, UC Berkeley

High resolution zone plate microscopy

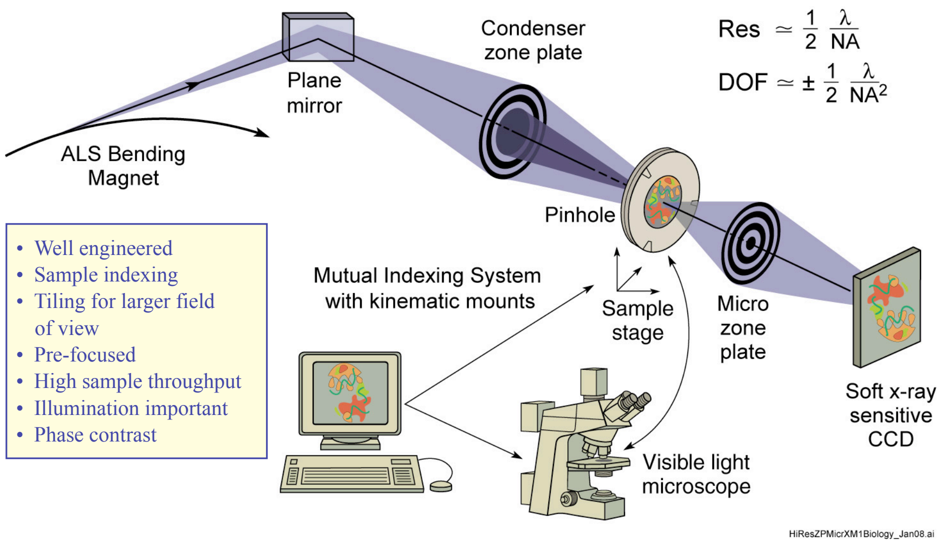

- Well engineered
- Sample indexing
- Tiling for larger field of view
- Pre-focused
- High sample throughput
- Illumination important
- Phase contrast

CheironSchool_Sept2011_Lec3.ppt 7

The water window for biological x-ray microscopy

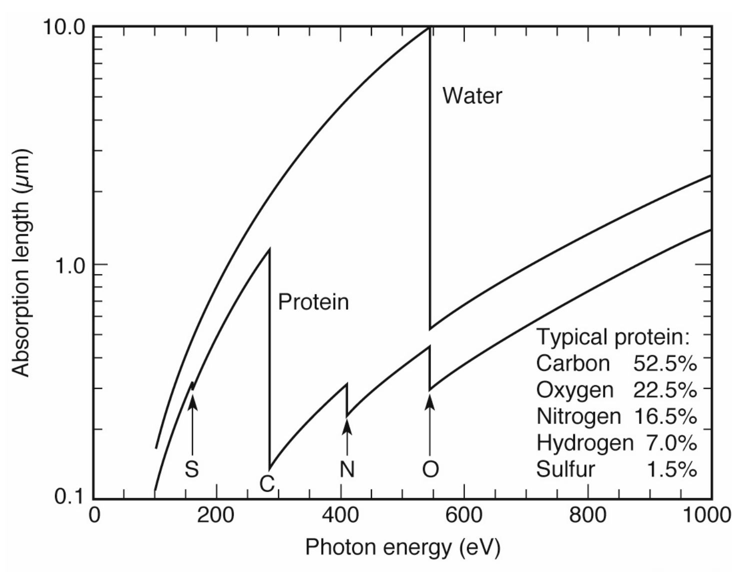

CheironSchool_Sept2011_Lec3.ppt 8

Fast freeze cryo fixation strongly mitigates radiation dose effects

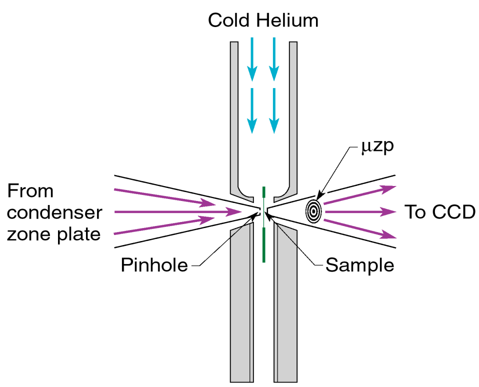

Helium passes through LN, is cooled, and directed onto sample windows

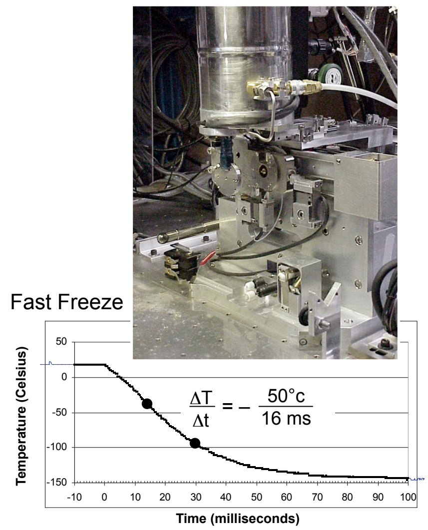

W. Meyer-Ilse, G. Denbeaux, L. Johnson, A. Pearson (CXRO-LBNL)

9 CheironSchool_Sept2011_Lec3.ppt

Organelle details imaged with cryogenic preservation and high spatial resolution

Cryo x-ray microscopy of 3T3 fibroblast cells

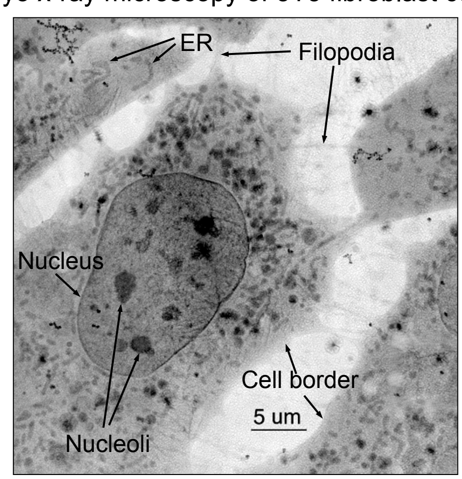

C. Larabell, D. Yager, D. Hamamoto, M. Bissell, T. Shin (LBNL Life Sciences Division)
W. Meyer-Ilse, G. Denbeaux, L. Johnson, A. Pearson (CXRO-LBNL)

10 CheironSchool_Sept2011_Lec3.ppt

Bending magnet radiation used with a soft x-ray microscope to form a high resolution image of a whole, hydrated mouse epithelial cell

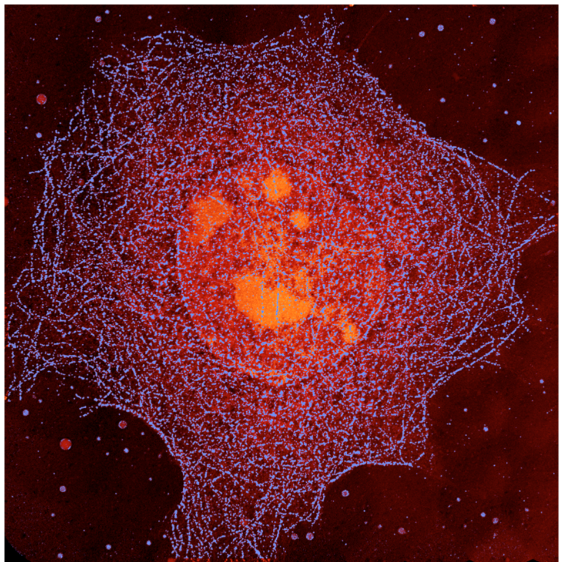

$\hbar\omega$ = 520 eV

32 μm x 32 μm

Ag enhanced Au labeling of the microtubule network, color coded blue.

Cell nucleus and nucleoli, moderately absorbing, coded orange.

Less absorbing aqueous regions coded black.

W. Meyer-Ilse et al.
J. Microsc. <u>201</u>, 395 (2001)

Courtesy of C. Larabell and W. Meyer-Ilse (LBNL)

11
CheironSchool_Sept2011_Lec3.ppt

Bio-nanotomography for 3D imaging of cells

Nanotomography of Cryogenic Fixed Cells

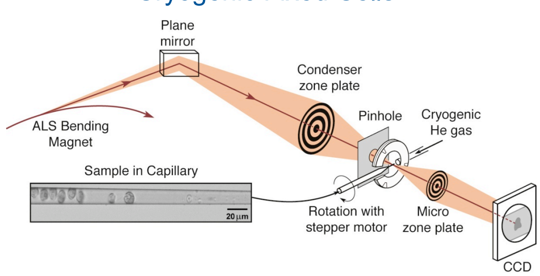

Courtesy of G. Schneider (BESSY)
Surf. Rev. Lett. <u>9</u>, 177 (2002)

Soft X-Ray Nanotomography of a Yeast Cell

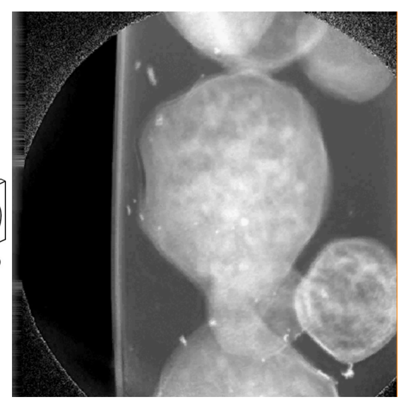

λ = 2.4 nm

Courtesy of C. Larabell (UCSF & LBNL) and M. LeGros (LBNL)

UCSF NCXT

12
CheironSchool_Sept2011_Lec3.ppt

Bio-nanotomography for 3D imaging of cells

Nanotomography of Cryogenic Fixed Cells

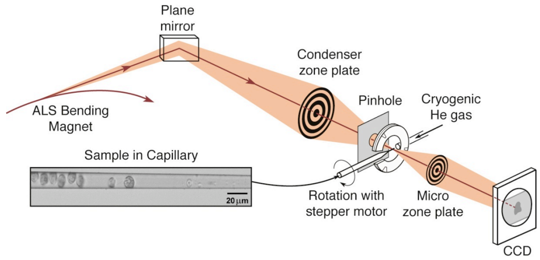

$\lambda = 2.4$ nm (517 eV)
$\Delta r = 35$ nm
$N = 320$
$NA = 0.034$
$D = 45$ μm
$f = 650$ μm
$\sigma = 0.64$
Resolution = 60 nm

Soft X-Ray Nanotomography of a Yeast Cell

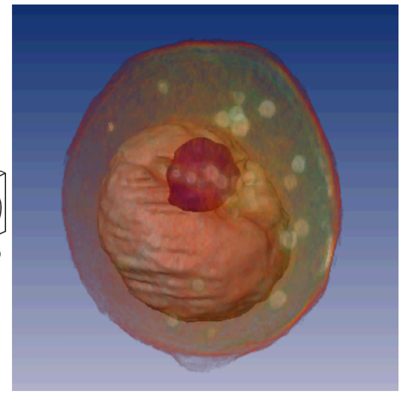

$\lambda = 2.4$ nm

Courtesy of C. Larabell (UCSF & LBNL) and M. LeGros (LBNL)

UCSF NCXT

13
CheironSchool_Sept2011_Lec3.ppt

Nanoscale 3-D biotomography

Mother daughter yeast cells just before separation

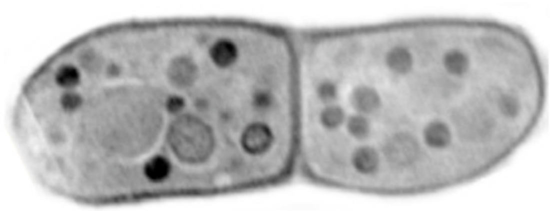

2-D slice from 3-D Tomogram. Images every 2°, 180° data set, several minutes. $\Delta r = 45$ nm

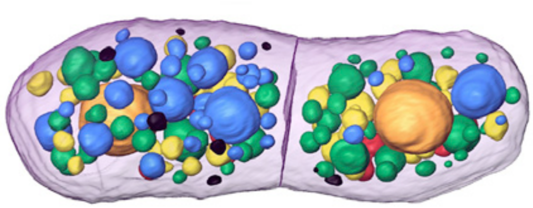

Color coding identifies subcellular components by their x-ray absorption coefficients

Courtesy of Carolyn Larabell, UCSF/LBNL.

14
CheironSchool_Sept2011_Lec3.ppt

Applications of soft x-ray microscopy

Biotomography at 60 nm resolution

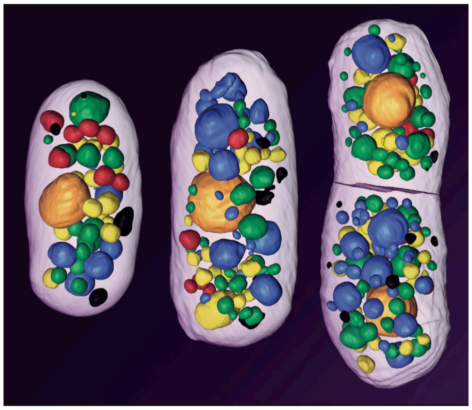

- Cryofixation
- 2° angular intervals
- Depth of focus limits resolution
- New XM-2 dedicated to biological applications, will become major facility worldwide to draw biologists to this evolving capability

Courtesy of C. Larabell (UCSF & LBNL)

UCSF NCXT

15 CheironSchool_Sept2011_Lec3.ppt

High resolution (30 nm), 3D image of a mouse cell by soft x-ray tomography

2D slice from 3D data set

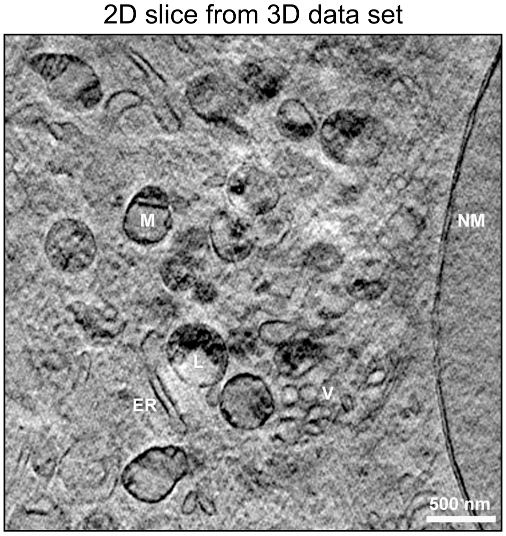

Details: 517 eV (2.4 nm)
Δr = 25 nm, 1° intervals, ±60°.
Note 29 nm nuclear membrane.

3D rendering

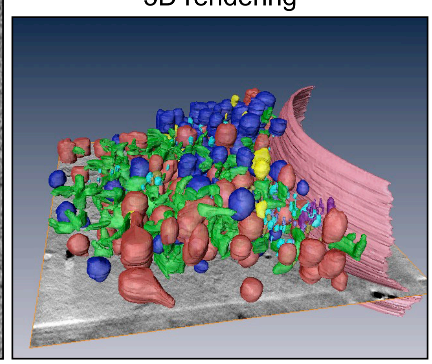

Courtesy of Gerd Schneider, BESSYII and James McNally, NIH.

16 CheironSchool_Sept2011_Lec3.ppt

Magnetic x-ray microscopy using x-ray magnetic circular dichroism (XMCD)

Magnetic X-Ray Microscopy

- **High spatial resolution in transmission**
- **Bulk sensitive (thin films)**
- **Complements surface sensitive PEEM**
- **Good elemental sensitivity**
- **Good spin-orbit sensitivity**
- **Allows applied magnetic field**
- **Insensitive to capping layers**
- **In-plane and out-of-plane measurements**

100 nm lines & spaces

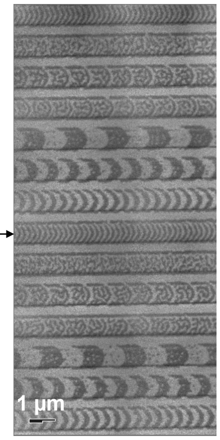

Courtesy of P. Fischer, (MPI, Stuttgart) and G. Denbeaux (CXRO/LBNL)

CheironSchool_Sept2011_Lec3.ppt 17

Magnetic domains imaged at different photon energies

FeGd Multilayer

Contrast reversal

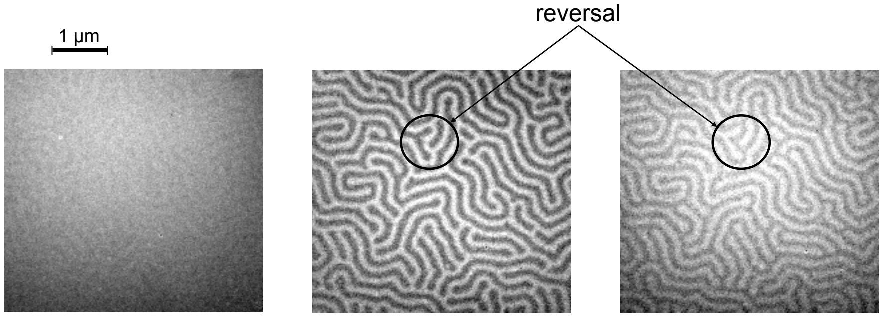

ħω = 704 eV below Fe L-edges | ħω = 707.5 eV Fe L_3-edge | ħω = 720.5 eV Fe L_2-edge

P. Fischer, T. Eimueller, M. Koehler (U. Wuerzberg)
S. Tsunashima (U. Nagoya) and N. Tagaki (Sanyo)
G. Denbeaux, L. Johnson, A. Pearson (CXRO-LBNL)

CheironSchool_Sept2011_Lec3.ppt 18

Magnetic recording of nanomagnetic patterns to 15 nm spatial resolution

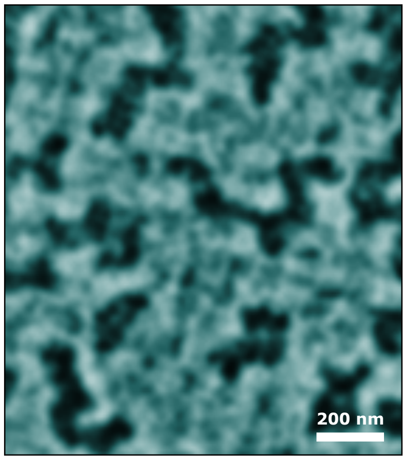

CoCrPt alloy
Co L_3-edge at 778 eV
(1.59 nm)

Courtesy of Peter Fischer (LBNL)

P. Fischer et al., *Mat. Today* 9, 26 (2006).

Time resolved studies of vortex dynamics in patterned permalloy thin films

Pump and Probe setup requires:
- Pump: Current pulse to “pump” sample
- Probe: X-ray pulses (70ps) from ALS 2 Bunch mode
- Perfect repeatability of dynamics

Sample:
50 nm thick 2μmx4μm permalloy ($Ni_{80}Fe_{20}$)
100nm thick gold waveguide
(ΔI along waveguide generates field to pump sample)

B.L. Mesler, P. Fischer, W. Chao, E. H. Anderson, D.H. Kim J. Vac. Sci. Technol. B 25, 2598 (2007).

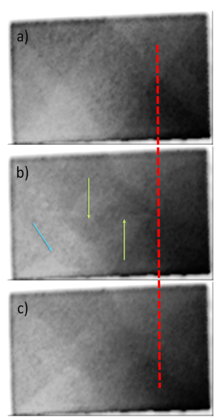

Before Pump (t=0)

t=+1 ns

t=+1.6 ns

Differential interference contrast (DIC) imaging at nanoscale magnetic edges

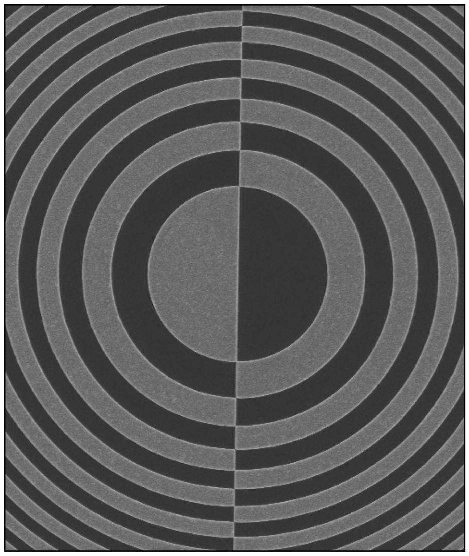

XOR Zone plate

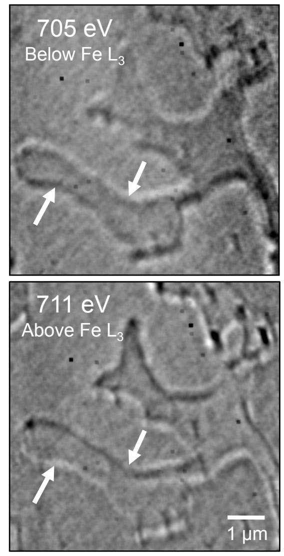

59 nm thick $Gd_{25}Fe_{75}$ layer

Courtesy of A. Sakdinawat, C. Chang and P. Fischer.

CheironSchool_Sept2011_Lec3.ppt 21

Environmental Consequences of Portland cement

1.5 billion ton of cement

Generates 1.5 billion ton of CO_2

Responsible for 7% CO_2 production in the world

Problem!

Courtesy of Professor Paulo Monteiro, CEE, UC Berkeley

Nanoscale x-ray imaging of cement processes: early hydrates forming during the pre-induction period

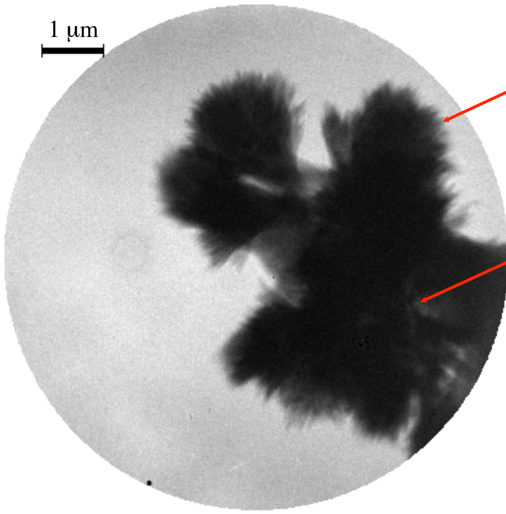

C3S hydrated for 34 min. in saturated lime and calcium sulfate at w/c = 5, 1 s exposure time, 516 eV, scale bar 1µm.

Courtesy of Professor Paulo Monteiro, CEE, UC Berkeley

Nanoscale x-ray imaging of cement processes

Calcium-Silicate-Hydrate (C-S-H): critical to cement strength and durability.

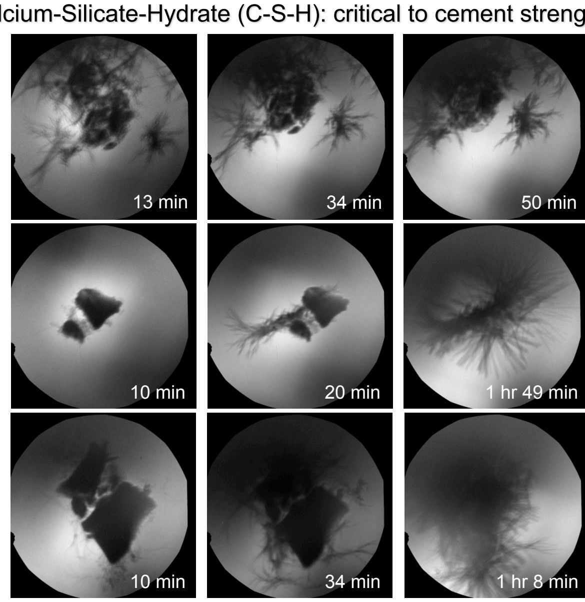

Orth C_3A

Orth C_3A + 1% $CaCl_2$

Orth C_3A + accelerator

C: carbon
Ca: calcium
A: alumina (Al_2O_3)
S: silica (SiO_2)

520 eV, 40 nm – spatial resolution

Courtesy of Professor Paulo Monteiro, CEE, UC Berkeley

24

Spectromicroscopy: high spatial and high spectral resolution of surface and thin films

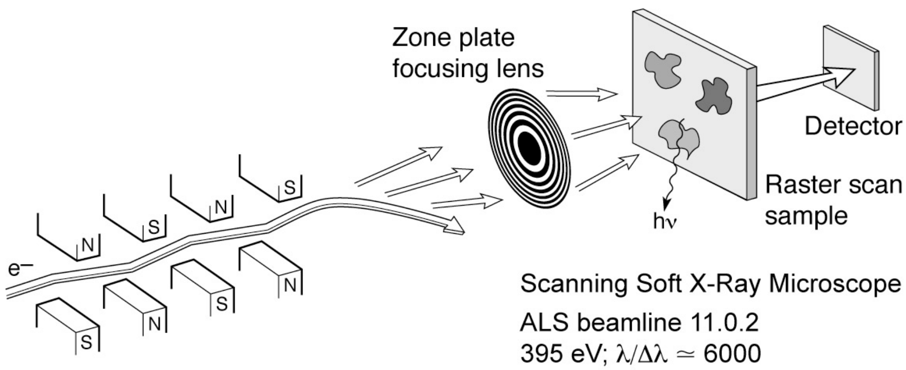

Scanning Soft X-Ray Microscope

ALS beamline 11.0.2
395 eV; $\lambda/\Delta\lambda \simeq 6000$
240 × 240 pixels
1.2 μm × 1.2 μm
2 ms dwell time

Ch09_F40a_Feb2010.ai

Biofilm from Saskatoon River

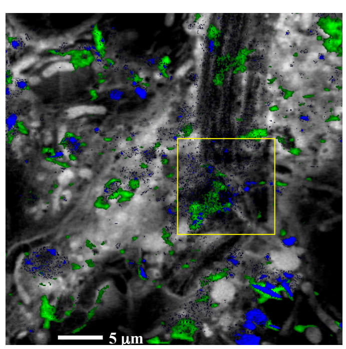

Protein (gray), Ca, K

RESULTS

- Ni, Fe, Mn, Ca, K, O, C elemental map, (there was no sign of Cr.)
- Different oxidation states for Fe and Ni

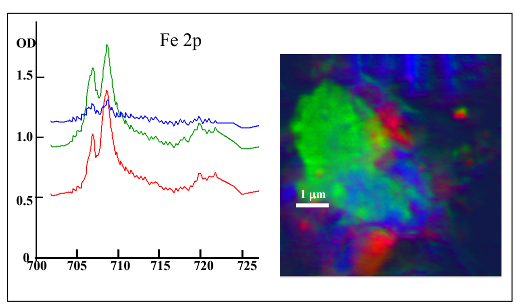

Different oxidation states (minerals) found for Fe & Ni

Tohru Araki, Adam Hitchcock (McMaster University)
Tolek Tyliszczak, LBNL
Sample from: John Lawrence, George Swerhone (NWRI-Saskatoon), Gary Leppard (NWRI-CCIW)

Patterned polymer photoresists

ALS-MES 11.0.2

M.K. Gilles, R. Planques, S.R. Leone
LBNL
Samples from B. Hinsberg, F. Huele
IBM Almaden

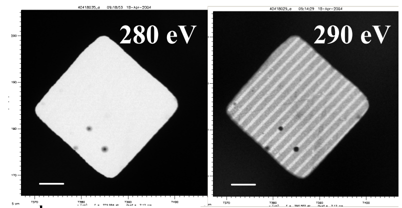

Exposure to UV light results in loss of carbonyl peak

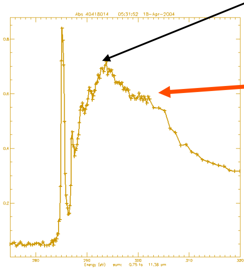

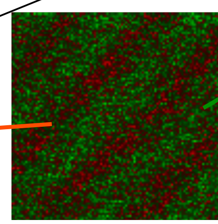

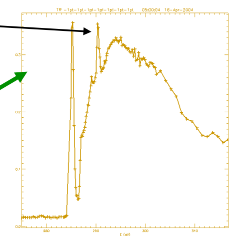

Map chemical spectra taken of pure samples onto a sample containing both components

Courtesy of Mary Gilles, LBNL

Hard x-ray zone plate microscopy

- Shorter wavelengths, potentially better spatial resolution and greater depth-of-field.
- Less absorption (β); phase shift (δ) dominates, higher efficiency.
- Thicker structures required (e.g., zones), higher aspect ratios pose nanofabrication challenges.
- Contrast of nanoscale samples minimal; will require good statistics, uniform background, dose mitigation.

nanoXCT: Schematic and Challenges

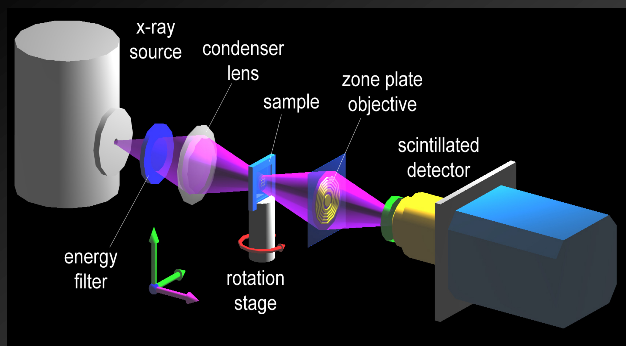

X-ray Zone-plate Lens

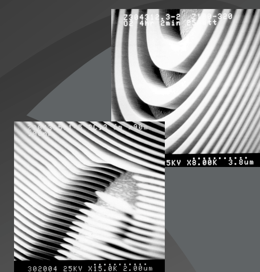

Challenges for achieving nm scale resolution:

- High resolution objective lens: limiting the ultimate resolution
- High numerical aperture condenser lens:
- Detector: high efficiency for lab. source and high speed for synchrotron sources
- Precision mechanical system

Courtesy of Wenbing Yun and Michael Feser, Xradia

29

Xradia nanoXCT: Sub-25 nm Hard X-ray Image

Xradia Resolution Pattern

- 50 nm bar width
- 150 nm thick Au
- 8keV x-ray energy
- 3rd diffraction order

F. Duewer, M. Tang,
G. C. Yin, W. Yun,
M. Feser, et al.

Xradia nano-XCT
8-50S installed at
NSRRC, Taiwan

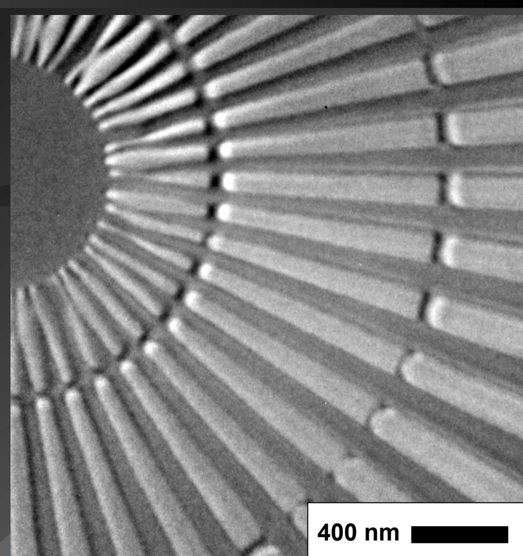

30

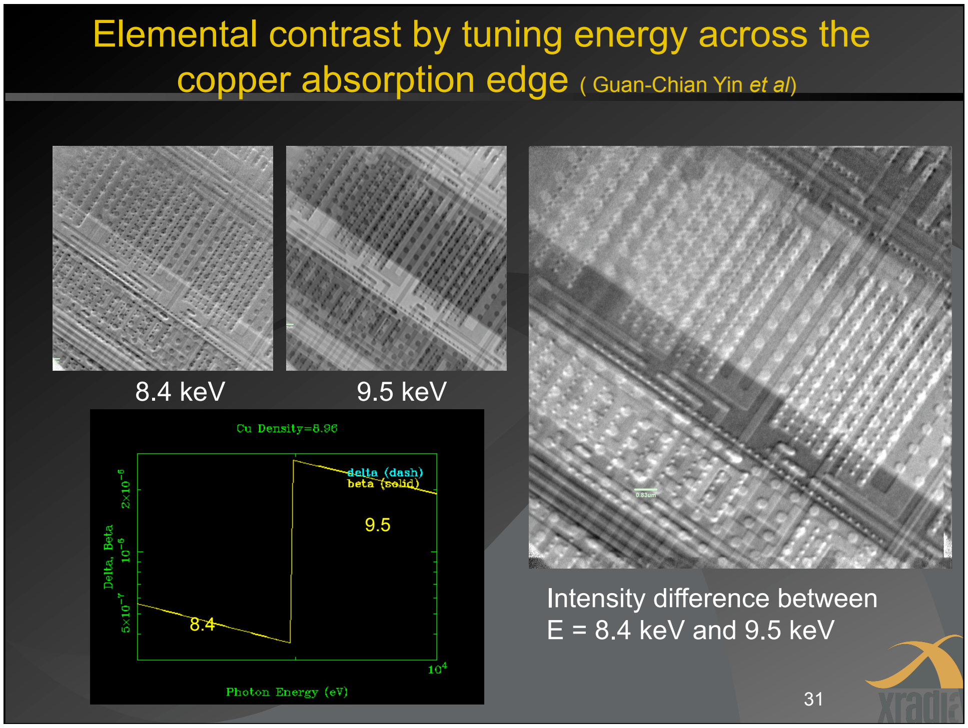
Elemental contrast by tuning energy across the copper absorption edge (Guan-Chian Yin et al)
8.4 keV
9.5 keV
Cu Density=8.96
delta (dash)
beta (solid)
9.5
8.4
Delta, Beta
Photon Energy (eV)
Intensity difference between
E = 8.4 keV and 9.5 keV
31

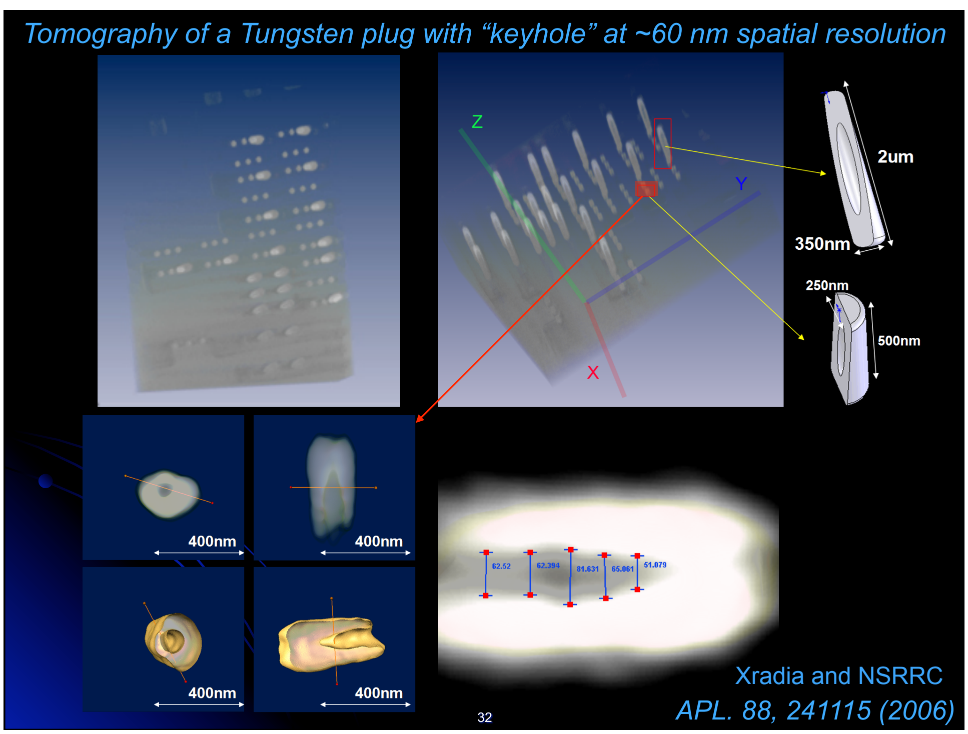
Tomography of a Tungsten plug with "keyhole" at ~60 nm spatial resolution
Z
Y
X
2um
350nm
250nm
500nm
400nm
400nm
400nm
400nm
Xradia and NSRRC
APL. 88, 241115 (2006)
32

Scanning x-ray fluorescence microprobe (μ-XRF)

Kirkpatrick-Baez (KB) mirror pair

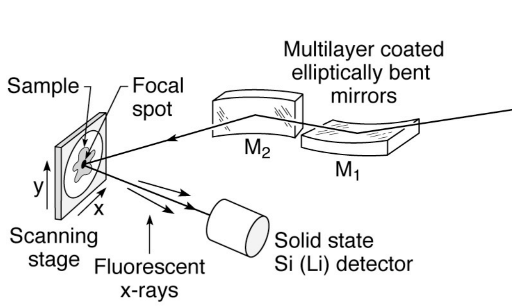

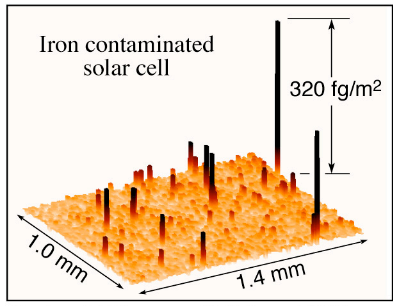

(Courtesy of A. Thompson and J. Underwood, LBNL; and R. Holm, Miles Lab)

FluoresMicroprobe_Sept2010.ai

- Crossed cylinders at glancing incidence
- Photon in / photon out, low noise background
- Femtogram and part per billion (ppb) sensitivity
- Micron focus (1988), now ~25 nm (Yamauchi, Mimura and colleagues, Osaka U./SPring-8)

J.H. Underwood and A.C. Thompson, NIM A266, 296 & 318 (1988).

CheironSchool_Sept2011_Lec3.ppt 33

X-ray microprobe at SPring-8

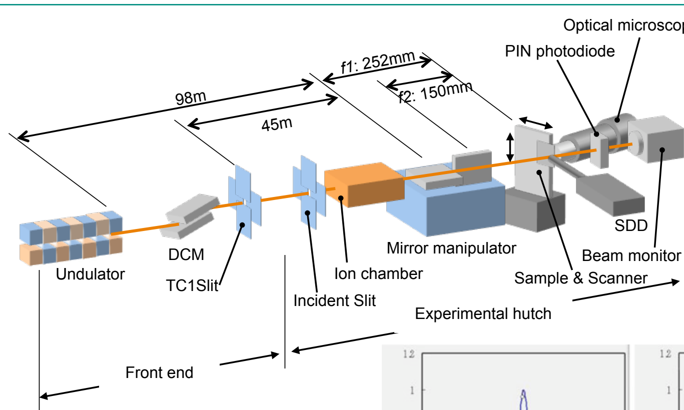

S. Matsuyama et al., Rev. Sci. Instrum. 77, 103102 (2006)

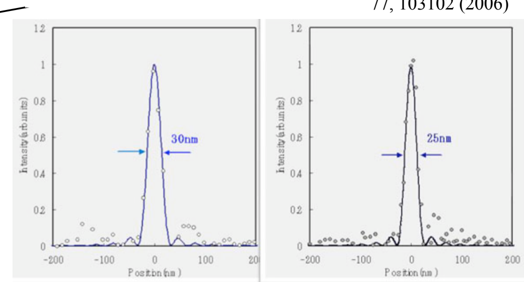

Courtesy of K. Yamauchi and H. Mimura, Osaka University.

34
CheironSchool_Sept2011_Lec3.ppt

Sub-cellular elemental analysis using the hard x-ray fluorescence microprobe at SPring-8

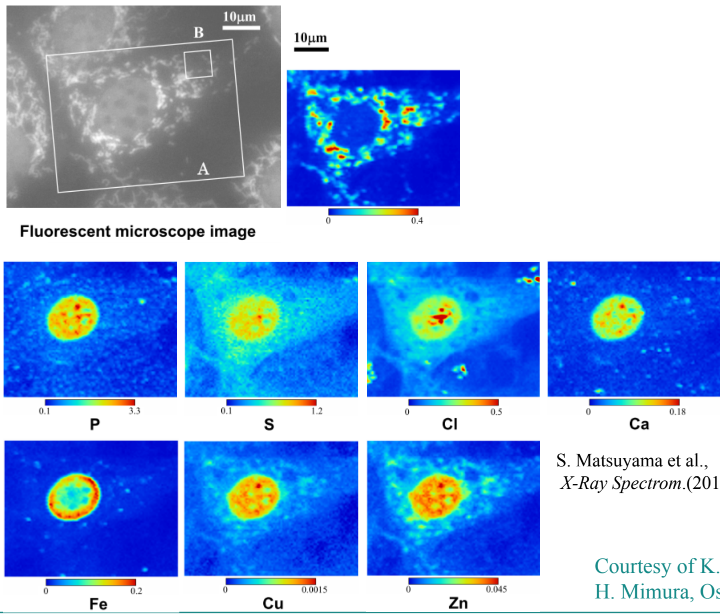

S. Matsuyama et al., *X-Ray Spectrom.*(2010).

Courtesy of K. Yamauchi and H. Mimura, Osaka University.

35 CheironSchool_Sept2011_Lec3.ppt

X-ray microprobe at SPring-8

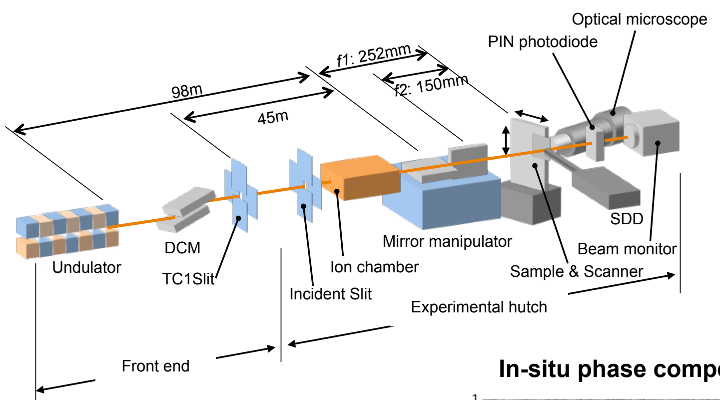

In-situ phase compensation

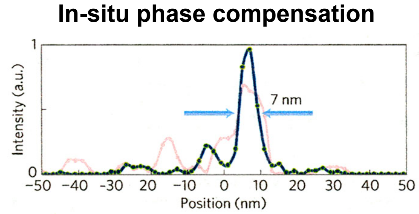

Courtesy of K. Yamauchi and H. Mimura, Osaka University.

H. Mimura et al., *Nature Physics*, **6**, 122 (2009)

36 CheironSchool_Sept2011_Lec3.ppt

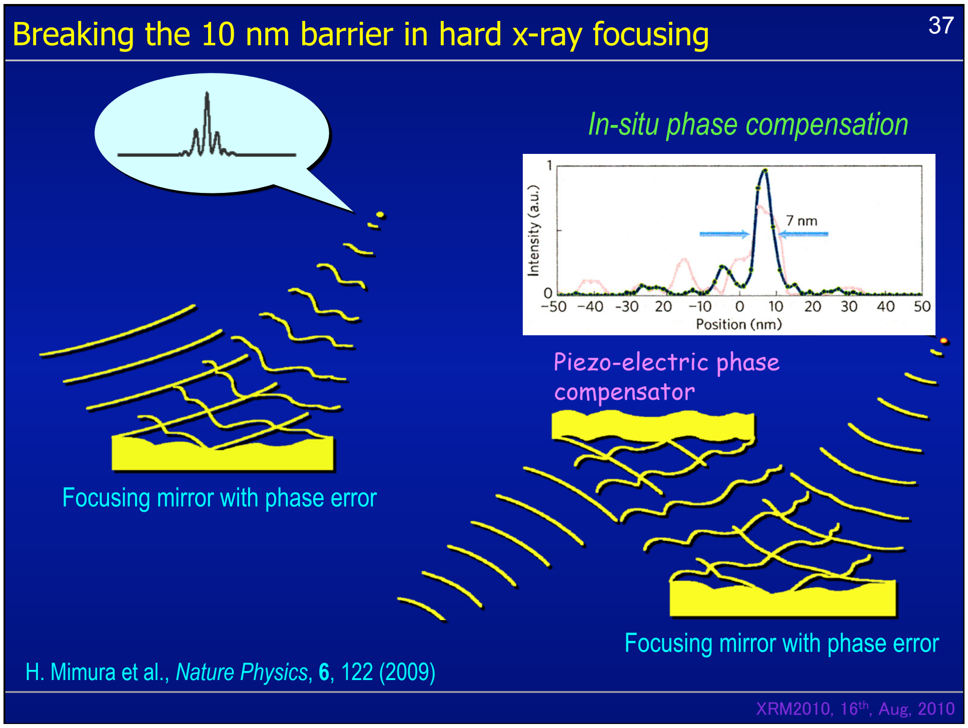
Breaking the 10 nm barrier in hard x-ray focusing
37
In-situ phase compensation
Intensity (a.u.)
7 nm
Position (nm)
Piezo-electric phase compensator
Focusing mirror with phase error
Focusing mirror with phase error
H. Mimura et al., Nature Physics, 6, 122 (2009)
XRM2010, 16th, Aug, 2010

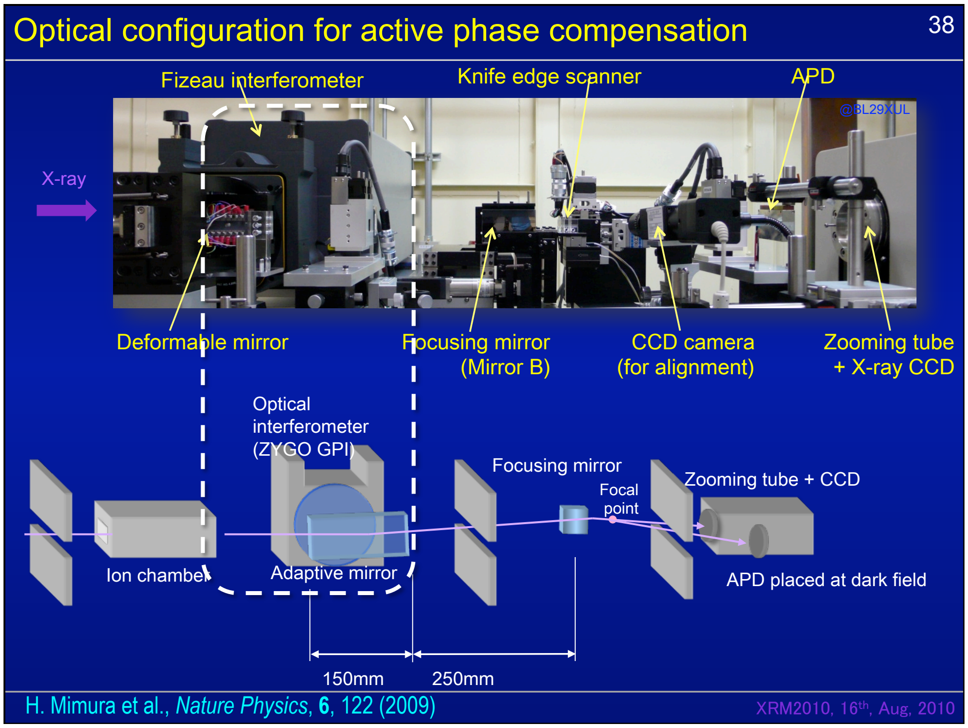
Optical configuration for active phase compensation
38
Fizeau interferometer
Knife edge scanner
APD
X-ray
Deformable mirror
Focusing mirror (Mirror B)
CCD camera (for alignment)
Zooming tube + X-ray CCD
Optical interferometer (ZYGO GPI)
Focusing mirror
Focal point
Zooming tube + CCD
Ion chamber
Adaptive mirror
APD placed at dark field
150mm
250mm
H. Mimura et al., Nature Physics, 6, 122 (2009)
XRM2010, 16th, Aug, 2010

Synchrotron-based art conservation at ESRF

μ-XRF, μ-XRD, μ-XANES

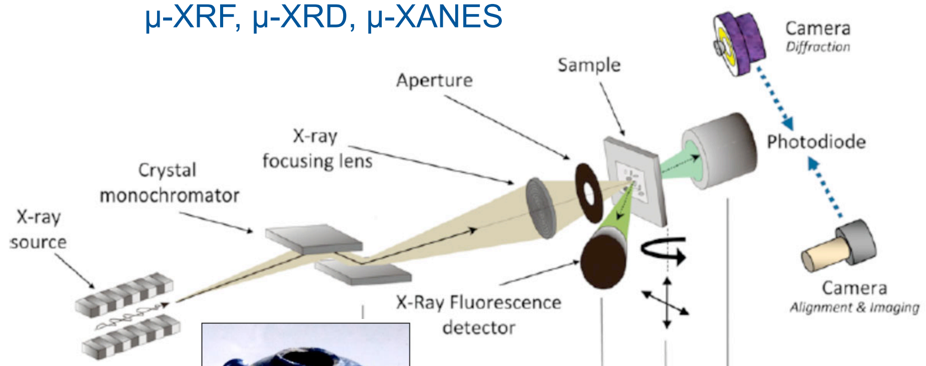

18th Dynasty Egyptian glass vase (1500 B.C.)

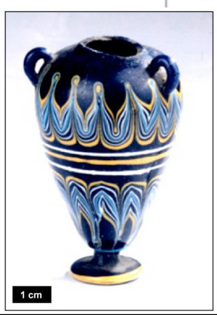

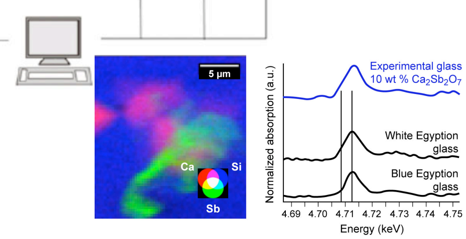

Courtesy of Marine Cotte (ESRF, Grenoble, France)

39

CheironSchool_Sept2011_Lec3.ppt

Examples of μ-XANES K-edge spectra occurring in art materials

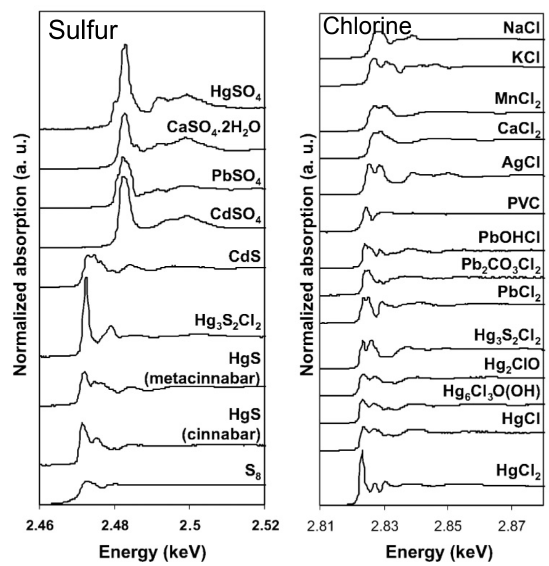

Courtesy of Marine Cotte (ESRF, Grenoble, France)

40

CheironSchool_Sept2011_Lec3.ppt

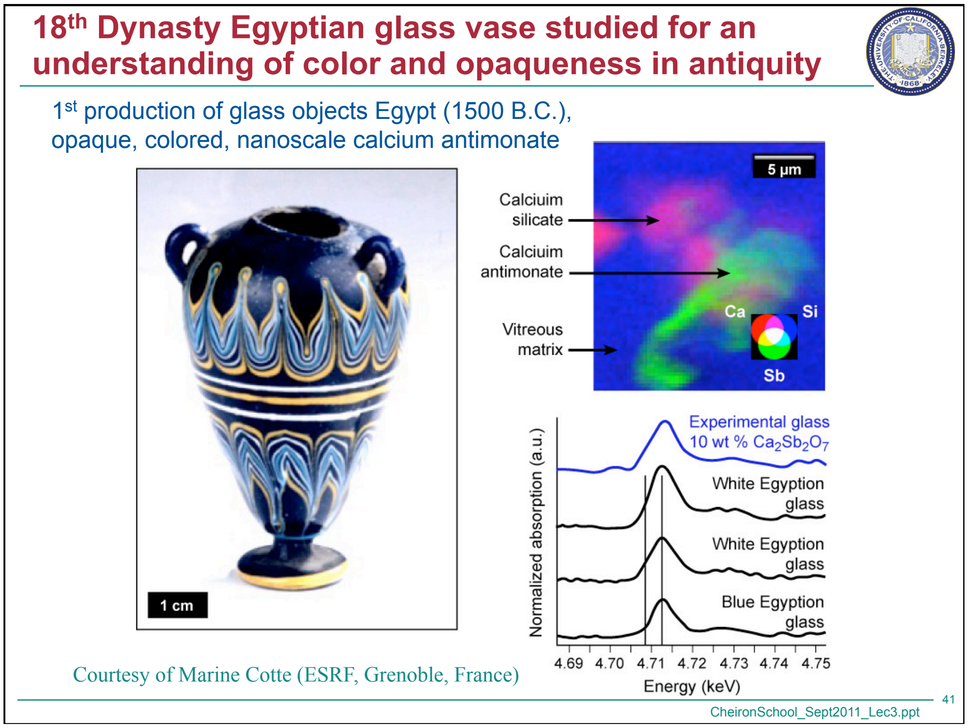
18th Dynasty Egyptian glass vase studied for an understanding of color and opaqueness in antiquity
1st production of glass objects Egypt (1500 B.C.), opaque, colored, nanoscale calcium antimonate
1 cm
5 µm
Calciuim silicate
Calciuim antimonate
Vitreous matrix
Ca
Si
Sb
Experimental glass
10 wt % $Ca_2Sb_2O_7$
White Egyption glass
White Egyption glass
Blue Egyption glass
Normalized absorption (a.u.)
4.69 4.70 4.71 4.72 4.73 4.74 4.75
Energy (keV)
Courtesy of Marine Cotte (ESRF, Grenoble, France)
41
CheironSchool_Sept2011_Lec3.ppt

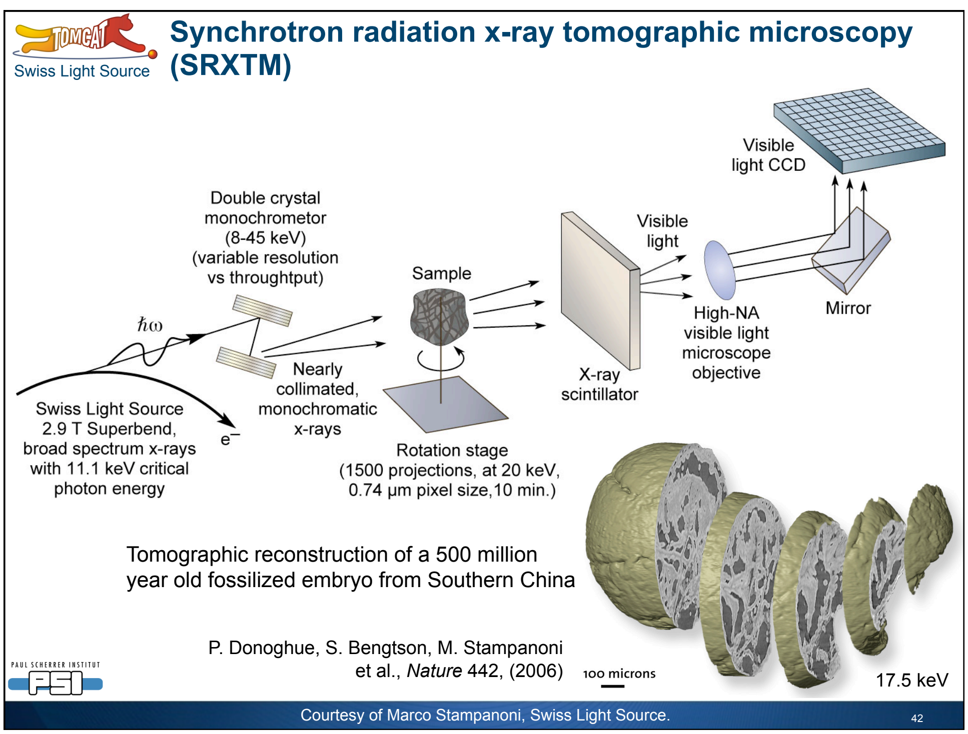
TOMCAT
Swiss Light Source
Synchrotron radiation x-ray tomographic microscopy (SRXTM)
Visible light CCD
Double crystal monochrometor (8-45 keV) (variable resolution vs throughtput)
Visible light
Sample
$\hbar\omega$
High-NA visible light microscope objective
Mirror
Nearly collimated, monochromatic x-rays
X-ray scintillator
Swiss Light Source 2.9 T Superbend, broad spectrum x-rays with 11.1 keV critical photon energy
e−
Rotation stage (1500 projections, at 20 keV, 0.74 µm pixel size,10 min.)
Tomographic reconstruction of a 500 million year old fossilized embryo from Southern China
P. Donoghue, S. Bengtson, M. Stampanoni et al., *Nature* 442, (2006)
100 microns
17.5 keV
PAUL SCHERRER INSTITUT
PSI
Courtesy of Marco Stampanoni, Swiss Light Source.
42

Swiss Light Source

Tomographic reconstruction of a 500 million year old fossilized embryo from Southern China

Markelia hunanensis
relative of modern roundworms and arthropods

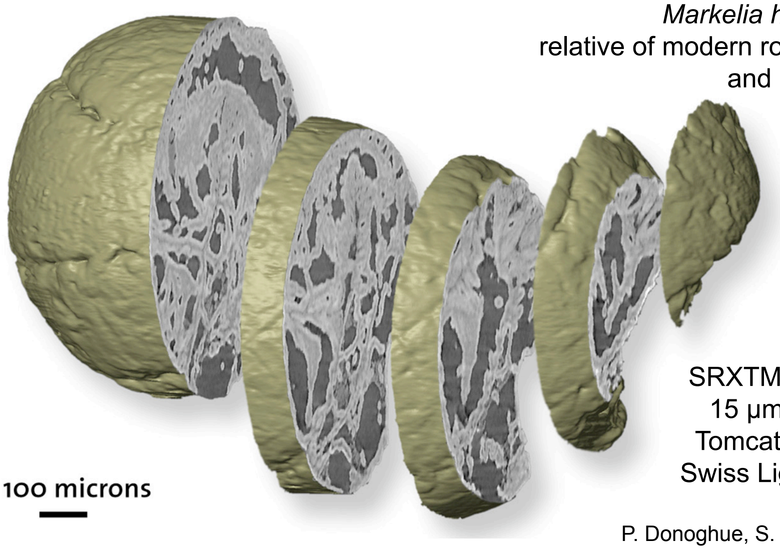

100 microns

SRXTM, 17.5 keV,
15 μm resolution
Tomcat Beamline,
Swiss Light Source

P. Donoghue, S. Bengtson, M. Stampanoni et al., *Nature* 442, (2006)

PAUL SCHERRER INSTITUT

Courtesy of Marco Stampanoni, Swiss Light Source. 43

Swiss Light Source

TOMCAT Microscope

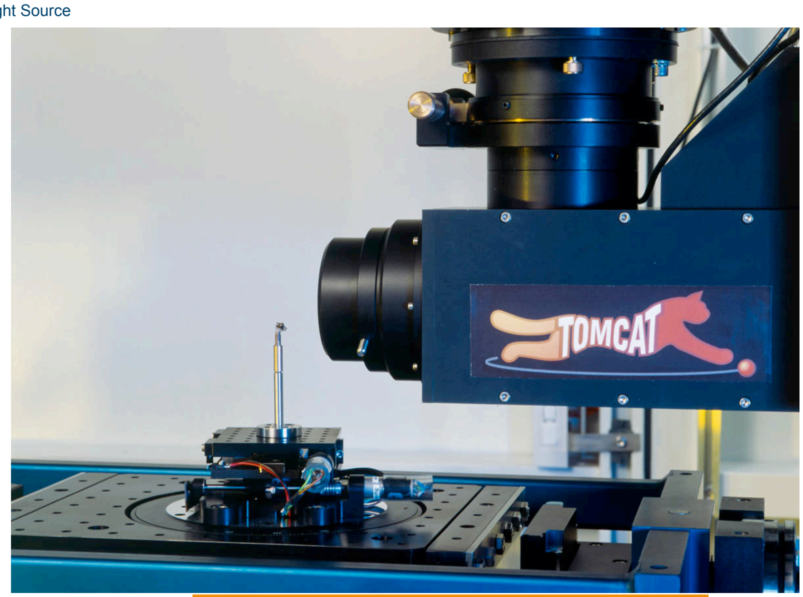

1 micron @ 10% MTF reached routinely

PAUL SCHERRER INSTITUT

Courtesy of Marco Stampanoni, Swiss Light Source. 44

Swiss Light Source

TOMCAT Microscope

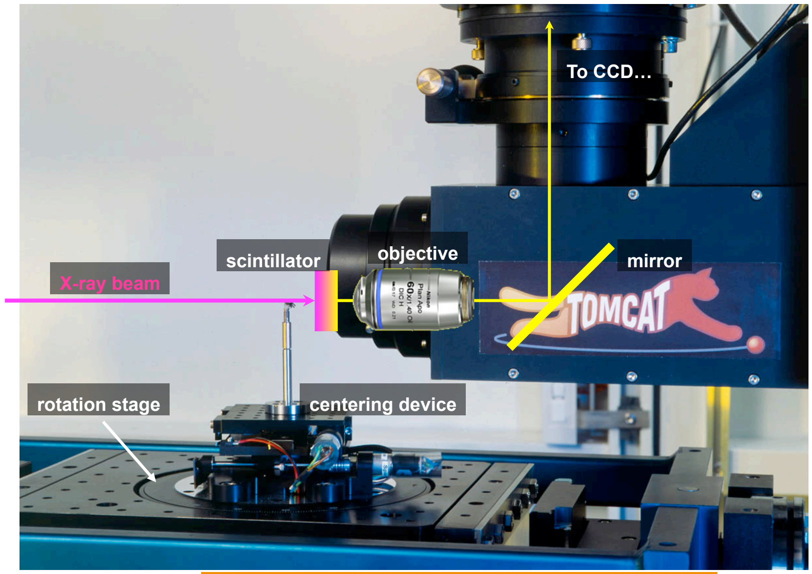

1 micron @ 10% MTF reached routinely

PAUL SCHERRER INSTITUT PSI

Courtesy of Marco Stampanoni, Swiss Light Source. 45

Swiss Light Source

Hard x-ray 3D x-ray tomography: microvascular architecture of a mouse brain

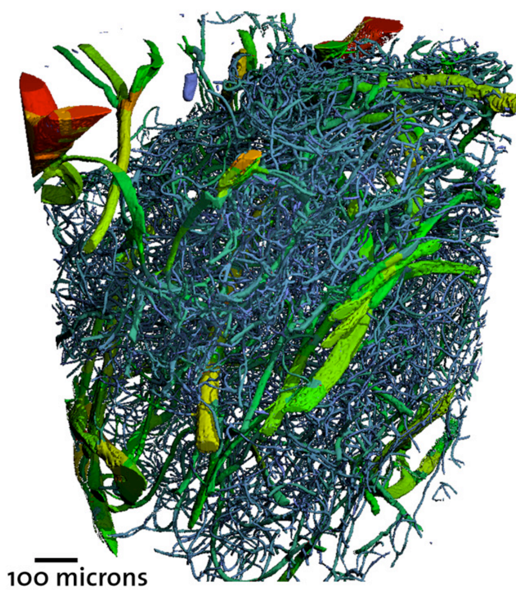

SRXTM, 25 keV,
15 μm resolution
Tomcat Beamline,
Swiss Light Source

M. Stampanoni,
T. Krucker et al.,
Adv. Neur. Res. (2008)

PAUL SCHERRER INSTITUT PSI

Courtesy of Marco Stampanoni, Swiss Light Source. 46

A lens is not necessarily required

$\Delta r_{resol.} = k_1 \lambda / NA$

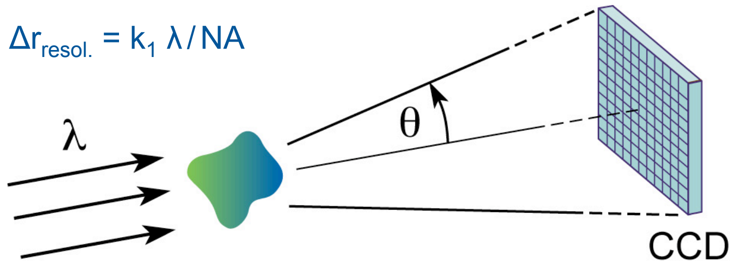

"Lensless" coherent diffraction imaging (CDI) is being aggressively pursued.

Coherent diffractive imaging (CDI)

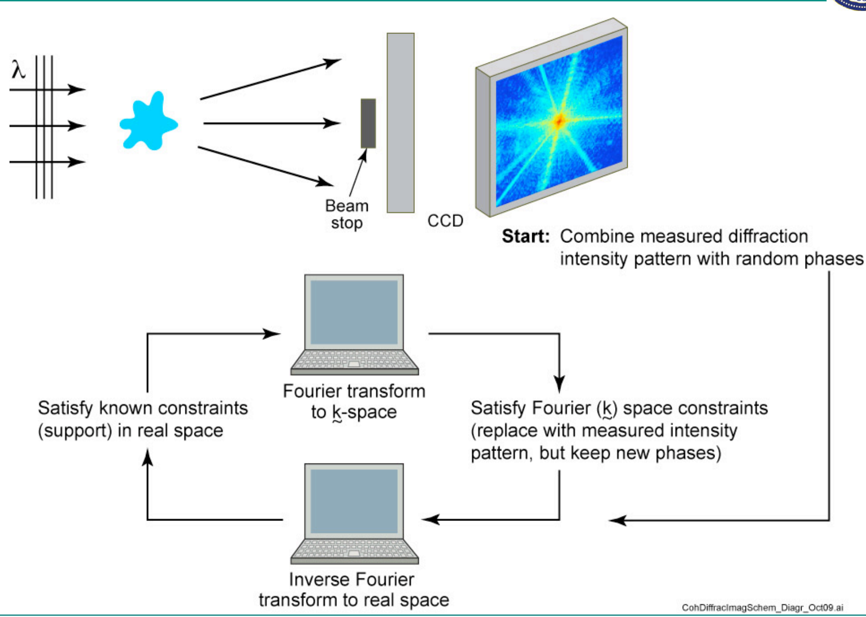

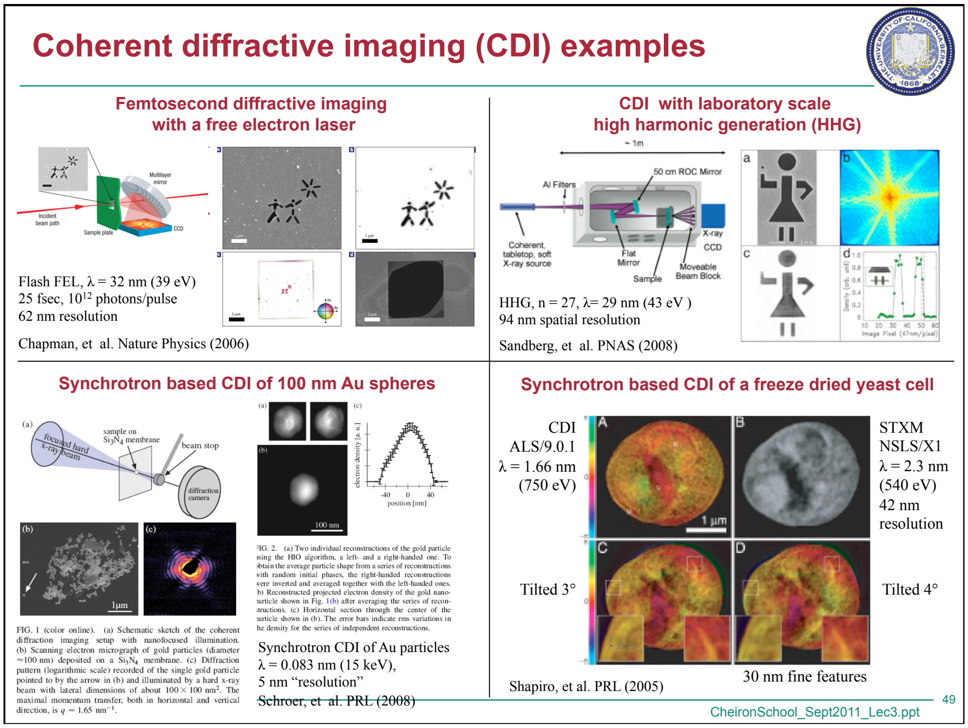
Coherent diffractive imaging (CDI) examples
Femtosecond diffractive imaging with a free electron laser
Flash FEL, λ = 32 nm (39 eV)
25 fsec, 10^12 photons/pulse
62 nm resolution
Chapman, et al. Nature Physics (2006)
CDI with laboratory scale high harmonic generation (HHG)
HHG, n = 27, λ= 29 nm (43 eV)
94 nm spatial resolution
Sandberg, et al. PNAS (2008)
Synchrotron based CDI of 100 nm Au spheres
Synchrotron CDI of Au particles
λ = 0.083 nm (15 keV),
5 nm "resolution"
Schroer, et al. PRL (2008)
Synchrotron based CDI of a freeze dried yeast cell
CDI
ALS/9.0.1
λ = 1.66 nm
(750 eV)
STXM
NSLS/X1
λ = 2.3 nm
(540 eV)
42 nm
resolution
Tilted 3°
Tilted 4°
30 nm fine features
Shapiro, et al. PRL (2005)
49
CheironSchool_Sept2011_Lec3.ppt

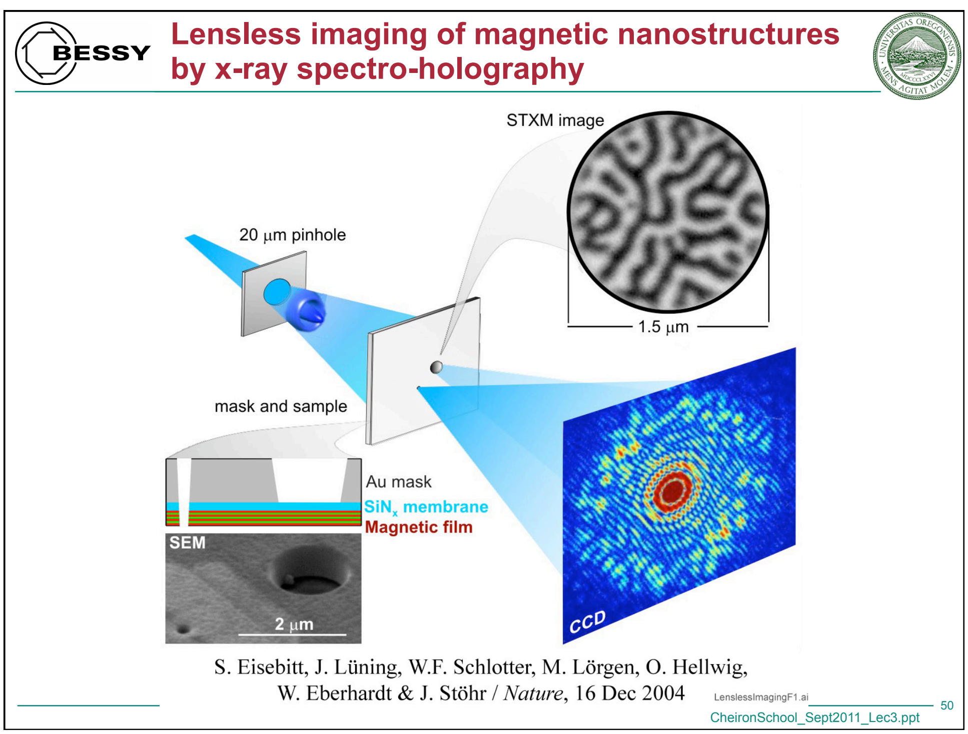
BESSY
Lensless imaging of magnetic nanostructures by x-ray spectro-holography
STXM image
20 μm pinhole
1.5 μm
mask and sample
Au mask
SiNx membrane
Magnetic film
SEM
2 μm
CCD
S. Eisebitt, J. Lüning, W.F. Schlotter, M. Lörgen, O. Hellwig,
W. Eberhardt & J. Stöhr / Nature, 16 Dec 2004
LenslessImagingF1.ai
50
CheironSchool_Sept2011_Lec3.ppt

Lectures online at www.youtube.com

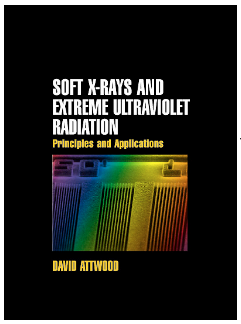

Amazon.com

UC Berkeley
www.coe.berkeley.edu/AST/sxreuv
www.coe.berkeley.edu/AST/srms
www.coe.berkeley.edu/AST/sxr2009

51
CheironSchool_Sept2011_Lec3.ppt